

Title: Asymptotics of the eprl model on arbitrary vertices

Speakers: Simone Speziale

Series: Quantum Gravity

Date: May 14, 2020 - 3:00 PM

URL: <http://pirsa.org/20050020>

Abstract: We introduce a new technique to study the critical point equations of the eprl model. We show that it correctly reproduces the 4-simplex asymptotics, and how to apply it to an arbitrary vertex. We find that for general vertices, the asymptotics can be linked to a Regge action for polytopes, but contain also more general geometries, called conformal twisted geometries. We present explicit examples including the hypercube, and discuss implications.

The asymptotic analysis of the Lorentzian EPRL-KKL vertex of arbitrary valence

Simone Speziale
Virtual PI seminar
14 mai 2020

Based on

P. Donà, M. Fanizza, G. Sarno and SiS, *SU(2) graph invariants, Regge actions and polytopes*
(1708.01727)

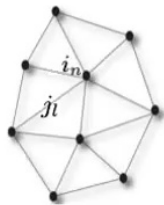
and

P. Donà and SiS, *Asymptotics of the Lorentzian EPRL-KKL amplitude for general vertices*
to appear (monday unless your questions tonight prove everything wrong...)



One path for the semiclassical limit of loop quantum gravity

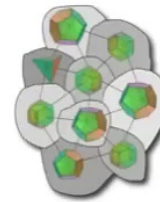
On a fixed graph:



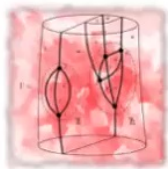
Spin networks



Twisted geometries



dynamics



Spin foams



(exp. of) Regge action “ $\int \mathcal{D}g_{\Delta} e^{iS_{\text{Regge}}(g_{\Delta})}$ ”

Then study refinement to increase number of degrees of freedom to relevant physical question...

The screenshot shows a Keynote presentation window titled 'PI20.key'. The main slide is titled 'Outline of the talk' in red. It contains a bulleted list of topics. The left sidebar shows a list of 8 slides, with slide 3 highlighted. The right sidebar shows the 'Slide Layout' panel with a 'Blank' layout selected and an 'Edit Master Slide' button.

Outline of the talk

- There exist a covariant framework for the dynamics of LQG, known as *spin foam formalism*
- State of the art: the EPRL model
- This is particularly developed in the case of 4-valent spin networks, which are dual to 3d simplicial triangulations and presents a simple interpretation in terms of *discrete* geometries
- For these, the spin foam amplitude for one 4-simplex is dominated in the semiclassical limit by exponentials of the **Regge action**
- Quite a nice state of affair, even though much more work is needed
(*notably on the semiclassical limit of an extended triangulation and curved solutions*)
- An open question is the semiclassical limit for non-simplicial vertices
relevant since the LQG Hilbert space contains a priori states of **any valency**

Kaminski-Kisielowski-Lewandowski: Spin-Foams for All Loop Quantum Gravity 0909.0939
Ding-Han-Rovelli: Generalized Spinfoams 1011.2149

PI20.key

View Zoom Add Slide Play Keynote Live Table Chart Text Shape Media Comment Collaborate Format Animate Document

EPRL general vertex amplitude

The EPRL vertex amplitude is a real function associated to any oriented graph with N nodes and L links:

$$A_{\Gamma}(j_{ab}, m_{ab}, n_{ab}) = \int \prod_{a=2}^N dh_a \prod_{(ab)} D_{j_{ab} m_{ab} j_{ab} n_{ab}}^{(\gamma j_{ab}, j_{ab})} (h_a^{-1} h_b)$$

Coherent vertex amplitude: replace the $SU(2)$ magnetic numbers with $SU(2)$ coherent states
 An idea born at PI... (Livine-S '07)

In the limit when all spins are large, the coherent amplitude decays exponentially, except for special configurations where the decay is power law.
The special configurations admit an interesting geometric interpretation, and so does their frequency of oscillations

The model uses only the 'γ-simple' representations defined by the Y-map:

$$(\rho_{ab}, k_{ab}), \quad \rho_{ab} = \gamma k_{ab}, \quad j_{ab} \geq k_{ab} \equiv k_{ab}$$

The saddle point analysis with non-simple representations is harder
 With the simple ones, it is almost as easy as for the Euclidean or BF models
 The results are also very similar, except for the main difference that Lorentzian boundary data can have power-law behaviour

Slide Layout

Blank

Change Master

Appearance

☐ Title

☐ Body

☐ Slide Number

► Background

Edit Master Slide

PI20.key

View Zoom Add Slide Play Keynote Live Table Chart Text Shape Media Comment Collaborate Format Animate Document

Two sets of spinors

- The infinite-dimensional unitary irreps of the principal series can be realized on \mathbb{C}^2

$$A_\Gamma(j_{ab}, m_{ab}, n_{ab}) = \int \prod_{a=2}^N dh_a \prod_{(ab)} D_{j_{ab} m_{ab} j_{ab} n_{ab}}^{(\gamma j_{ab}, j_{ab})}(h_a^{-1} h_b)$$

$\Leftrightarrow D(h) = \text{integrals over spinors } z$
- The $SU(2)$ CS are more conveniently described by a spinor than a unit vector: ζ such that $\vec{n} = -\langle \zeta | \vec{\sigma} | \zeta \rangle$

Two advantages of using coherent states:

- introduce a finer characterization of the boundary data: an orthogonal intertwiner gives a maximally spread 3-geometry
- permit to factorize the explicit expressions for the matrix elements and write them as a single exponential

Coherent vertex amplitude:

$$A_\Gamma(j_{ab}, \vec{n}_{ab}, -\vec{n}_{ba}) = e^{i \sum_{(ab)} j_{ab} \psi_{ab}} \prod_{(ab)} \frac{d j_{ab}}{\pi} \int \prod_{a=2}^N dh_a \int \prod_{(ab)} \frac{d\mu(z_{ab})}{\|h_a^\dagger z_{ab}\|^2 \|h_b^\dagger z_{ab}\|^2} \exp S$$

$$S(h, z) = \sum_{(ab)} j_{ab} \log \frac{\langle h_a^\dagger z_{ab} | \zeta_{ab} \rangle^2 \langle \zeta_{ba} | h_b^\dagger z_{ab} \rangle^2}{\|h_a^\dagger z_{ab}\|^2 \|h_b^\dagger z_{ab}\|^2} - i \gamma j_{ab} \log \frac{\|h_a^\dagger z_{ab}\|^2}{\|h_b^\dagger z_{ab}\|^2}$$

- The action does not have a manifest link to (discrete) general relativity; so the classical dynamics of the model is open for investigations. One possibility is that a link to GR emerges in the large spin limit.
- The action is linear in the spins: large spin asymptotics can be studied using saddle point approximation

PI20.key

View Zoom Add Slide Play Keynote Live Table Chart Text Shape Media Comment Collaborate Format Animate Document

Saddle point approximation

Approximate the integrals with Gaussians around critical points of the action: $\partial S = 0$

Because the action is complex, critical points can have different real parts of the on-shell action

$$S^{(c)} = \text{Re}S^{(c)} + i \text{Im}S^{(c)}$$

- Those with maximal value of the real part will be exponentially dominating wrt the others
- Focus attention on the *maximal* critical points $\text{Re}S^{(c)} = \max$

This turns out to have a significant technical advantage:
the conditions for a maximal $\text{Re}(S)$ are simple to solve, and simplify in turns the gradient equations

With this condition, the **critical point equations** are:

- group element gradient: $\sum_{b \neq a} j_{ab} \vec{n}_{ab} = 0, \quad \forall a.$ restrictions on the boundary data
- spinor gradient: $\langle \zeta_{ab} | h_a^{-1} \vec{\sigma} h_a | \zeta_{ab} \rangle = [\zeta_{ba} | h_b^{-1} \vec{\sigma} h_b | \zeta_{ba}],$
 $[\zeta_{ba} | h_b^{-1} h_a | \zeta_{ab}] = \frac{[h_a^\dagger z_{ab}]}{[h_b^\dagger z_{ab}]} e^{i(v_{ab} - v_{ba})}.$ equations determining the h_a ;
they turn out to require additional
restrictions on the boundary data
else there are no solutions

phases for the z spinors

These and the max $\text{Re}(S)$ eqs. determine the spinors

PI20.key

View Zoom Add Slide Play Keynote Live Table Chart Text Shape Media Comment Collaborate Format Animate Document

Boosted orientation equations

The eqs determining the spinors are trivial. All the fun of the game is to determine the group elements. Focus on the group element eqs:

$$\langle \zeta_{ab} | h_a^{-1} \vec{\sigma} h_a | \zeta_{ab} \rangle = [\zeta_{ba} | h_b^{-1} \vec{\sigma} h_b | \zeta_{ba}]$$

First thing, let's get rid of the spinors.

Without loss of generality, we can rewrite these eqs in terms of vectors alone:

$$H_a \vec{n}_{ab} = -H_b \vec{n}_{ba} \quad \text{boosted orientation equations (BOE)}$$

where: $H \vec{n} := \langle \zeta | h^{-1} \vec{\sigma} h | \zeta \rangle$, $\vec{n} = -\langle \zeta | \vec{\sigma} | \zeta \rangle$

- H is the 3d (non-unitary) irrep of h
- explicitly, $\langle \zeta | h^{-1} \vec{\sigma} h | \zeta \rangle = \cosh r U \vec{n} - i \sinh r \vec{v} \times U \vec{n} + (1 - \cosh r)(\vec{v} \cdot U \vec{n}) \vec{v}$

This can be recognized as the Lorentz transformation of a self-dual bivector, with vanishing magnetic part and thus real self-dual part given by the vector n

The bivector can be written explicitly as $B_{IJ}^t := \epsilon_{IJKL} t^K n^L$

where we have introduced

$$t^I = (1, 0, 0, 0)$$

$$n^I := (0, \vec{n})$$

PI20.key

View Zoom Add Slide Play Keynote Live Table Chart Text Shape Media Comment Collaborate Format Animate Document

The role of the Y map

Why are such special bivectors popping out? $B_{IJ}^t := \epsilon_{IJKL} t^K n^L$

We are not just working with selected irreps of the Lorentz group

We are also selecting lowest weights in the basis diagonalizing the canonical SU(2) matrix subgroup (Y map)

It is this choices that introduces a preferred time-like direction, and selects this class of bivectors.

Slide Layout

Blank

Change Master

Appearance

☐ Title

☐ Body

☐ Slide Number

► Background

Edit Master Slide

The screenshot shows a Keynote presentation window titled "PI20.key". The main slide, titled "The obvious solution" in red, contains the following text:

There is an **obvious** solutions to the BOE $H_a \vec{n}_{ab} = -H_b \vec{n}_{ba}$

Consider a configuration with $\vec{n}_{ab} = -\vec{n}_{ba}$

\Rightarrow BOE solved by $H_a = 1$ for all nodes

The slide is part of a 9-slide deck. The right sidebar shows the "Slide Layout" panel with a "Blank" layout selected and a "Change Master" button. Below this, the "Appearance" panel has checkboxes for "Title", "Body", and "Slide Number", all of which are unchecked. A "Background" section is also visible with a white background selected. At the bottom of the sidebar is an "Edit Master Slide" button.

PI20.key

View Zoom Add Slide Play Keynote Live Table Chart Text Shape Media Comment Collaborate Format Animate Document

The obvious solution

There is an **obvious** solutions to the BOE $H_a \vec{n}_{ab} = -H_b \vec{n}_{ba}$

Consider a configuration with $\vec{n}_{ab} = -\vec{n}_{ba}$

⇒ BOE solved by $H_a = \mathbb{1}$ for all nodes

More generally, if the boundary normals satisfy $R_a \vec{n}_{ab} = -R_b \vec{n}_{ba}$, $R_a \in \text{SO}(3)$

⇒ BOE solved by $H_a = R_a \in \text{SO}(3)$ for all nodes

The non-trivial question is whether there exist additional solutions, and whether there are solutions with $H_a \notin \text{SO}(3)$

This is what requires all the work!

Boundary data satisfying \rightarrow were called **vector geometries** by Barrett

This is a good time to pause,
and take a detour on the geometry of the boundary data, regardless of the saddle point analysis

Slide Layout

Blank

Change Master

Appearance

☐ Title

☐ Body

☐ Slide Number

► Background

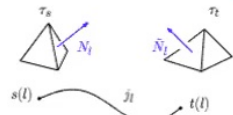
Edit Master Slide

[illegible]

- Generic data: a triple $(j_{ab}, \vec{n}_{ab}, \vec{n}_{ba})$ per link.
(A subset of the twisted geometry parametrization)

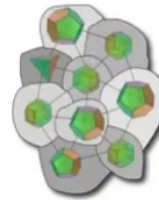
Classifying the boundary data: from 3d to 4d geometries

- Generic data: a triple $(j_{ab}, \vec{n}_{ab}, \vec{n}_{ba})$ per link.
(A subset of the twisted geometry parametrization)



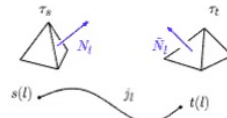
- Closed data: a collection of polyhedra dual to the nodes, with shape mismatch at the faces: twisted geometries

$$\sum_{b \neq a} j_{ab} \vec{n}_{ab} = 0, \quad \forall a.$$



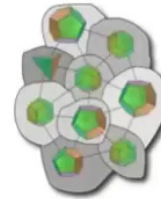
Classifying the boundary data: from 3d to 4d geometries

- Generic data: a triple $(j_{ab}, \vec{n}_{ab}, \vec{n}_{ba})$ per link.
(A subset of the twisted geometry parametrization)



- Closed data: a collection of polyhedra dual to the nodes, with shape mismatch at the faces: twisted geometries

$$\sum_{b \neq a} j_{ab} \vec{n}_{ab} = 0, \quad \forall a.$$



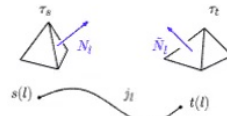
- Vector: a subset of twisted geometries satisfying the orientation conditions

$$R_a \vec{n}_{ab} = -R_b \vec{n}_{ba}, \quad R_a \in \text{SO}(3)$$



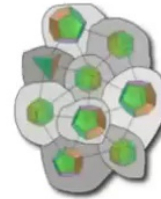
Classifying the boundary data: from 3d to 4d geometries

- Generic data: a triple $(j_{ab}, \vec{n}_{ab}, \vec{n}_{ba})$ per link.
(A subset of the twisted geometry parametrization)



- Closed data: a collection of polyhedra dual to the nodes, with shape mismatch at the faces: twisted geometries

$$\sum_{b \neq a} j_{ab} \vec{n}_{ab} = 0, \quad \forall a.$$



- Vector: a subset of twisted geometries satisfying the orientation conditions

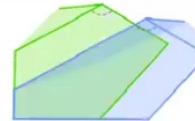
$$R_a \vec{n}_{ab} = -R_b \vec{n}_{ba}, \quad R_a \in \text{SO}(3)$$



- Conformal, or angle-matched: a subset of twisted geometries satisfying the angle-matching conditions

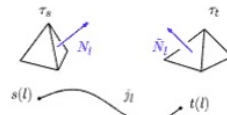
$$C_{1a,bc} := \frac{\cos \phi_{a1}^b + \cos \phi_{ab}^1 \cos \phi_{b1}^a}{\sin \phi_{ab}^1 \sin \phi_{b1}^a} - \frac{\cos \phi_{a1}^c + \cos \phi_{ac}^1 \cos \phi_{c1}^a}{\sin \phi_{ac}^1 \sin \phi_{c1}^a} = 0 \quad (\text{there are equivalent ways of writing them})$$

They can be split into Euclidean, and Lorentzian, according to the spherical cosine laws.
In the first case, they are a strict subset of vector geometries.



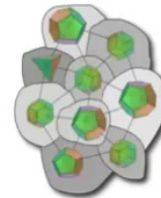
Classifying the boundary data: from 3d to 4d geometries

- Generic data: a triple $(j_{ab}, \vec{n}_{ab}, \vec{n}_{ba})$ per link.
(A subset of the twisted geometry parametrization)



- Closed data: a collection of polyhedra dual to the nodes, with shape mismatch at the faces: twisted geometries

$$\sum_{b \neq a} j_{ab} \vec{n}_{ab} = 0, \quad \forall a.$$



- Vector: a subset of twisted geometries satisfying the orientation conditions

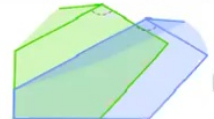
$$R_a \vec{n}_{ab} = -R_b \vec{n}_{ba}, \quad R_a \in \text{SO}(3)$$



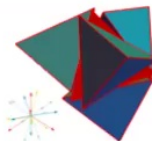
- Conformal, or angle-matched: a subset of twisted geometries satisfying the angle-matching conditions

$$C_{1a,bc} := \frac{\cos \phi_{a1}^b + \cos \phi_{ab}^1 \cos \phi_{b1}^a}{\sin \phi_{ab}^1 \sin \phi_{b1}^a} - \frac{\cos \phi_{a1}^c + \cos \phi_{ac}^1 \cos \phi_{c1}^a}{\sin \phi_{ac}^1 \sin \phi_{c1}^a} = 0 \quad (\text{there are equivalent ways of writing them})$$

They can be split into Euclidean, and Lorentzian, according to the spherical cosine laws.
In the first case, they are a strict subset of vector geometries.

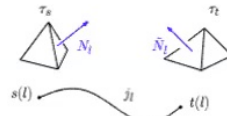


- 3d Regge: the subset satisfying full shape-matching conditions



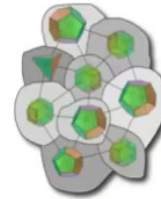
Classifying the boundary data: from 3d to 4d geometries

- Generic data: a triple $(j_{ab}, \vec{n}_{ab}, \vec{n}_{ba})$ per link.
(A subset of the twisted geometry parametrization)



- Closed data: a collection of polyhedra dual to the nodes, with shape mismatch at the faces: twisted geometries

$$\sum_{b \neq a} j_{ab} \vec{n}_{ab} = 0, \quad \forall a.$$



- Vector: a subset of twisted geometries satisfying the orientation conditions

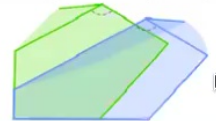
$$R_a \vec{n}_{ab} = -R_b \vec{n}_{ba}, \quad R_a \in \text{SO}(3)$$



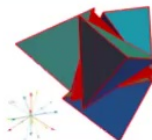
- Conformal, or angle-matched: a subset of twisted geometries satisfying the angle-matching conditions

$$C_{1a,bc} := \frac{\cos \phi_{a1}^b + \cos \phi_{ab}^1 \cos \phi_{b1}^a}{\sin \phi_{ab}^1 \sin \phi_{b1}^a} - \frac{\cos \phi_{a1}^c + \cos \phi_{ac}^1 \cos \phi_{c1}^a}{\sin \phi_{ac}^1 \sin \phi_{c1}^a} = 0 \quad (\text{there are equivalent ways of writing them})$$

They can be split into Euclidean, and Lorentzian, according to the spherical cosine laws.
In the first case, they are a strict subset of vector geometries.



- 3d Regge: the subset satisfying full shape-matching conditions



- Flat-embeddable 3d Regge: the subset that describes the boundary geometry of a 4d polytope



PI20.key

View 96% Zoom Add Slide Play Keynote Live Table Chart Text Shape Media Comment Collaborate Format Animate Document

More on conformal twisted geometries

They have two non-trivial geometric properties, that play a crucial role in the saddle point analysis:

- By having a well-defined valence for each face dual to the link, conformal twisted geometries introduce a map from cycles of the graph to edges of a cellular decomposition.
- They assign a unique 4d dihedral angle to each face, via the spherical cosine laws (SCL).

Slide Layout

Blank

Change Master

Appearance

☐ Title

☐ Body

☐ Slide Number

► Background

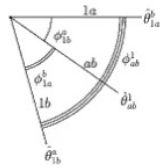
Edit Master Slide

Conformal twisted geometries and spherical cosine laws

For general data, we can define the 3d dihedral angles from the normals

$$\vec{n}_{ab} \cdot \vec{n}_{ac} = \cos \phi_{bc}^a$$

We can use them to define 4d dihedral angles via the spherical cosine laws (SCL)



$$\cos \hat{\theta}_{a1}^b = \frac{\cos \phi_{a1}^b + \cos \phi_{ab}^1 \cos \phi_{b1}^a}{\sin \phi_{ab}^1 \sin \phi_{b1}^a}$$

Range determined by the boundary data:

- >1 , Lorentzian, co-chronal (thick wedge)
- $[-1,1]$, Euclidean
- <-1 , Lorentzian, anti-chronal (thin wedge)

This definition depends on the edge chosen.

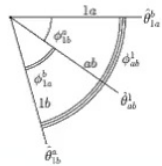
When the 2d angles match, the expression becomes independent of b , and defines a unique 4d angle

Conformal twisted geometries and spherical cosine laws

For general data, we can define the 3d dihedral angles from the normals

$$\vec{n}_{ab} \cdot \vec{n}_{ac} = \cos \phi_{bc}^a$$

We can use them to define 4d dihedral angles via the spherical cosine laws (SCL)



$$\cos \hat{\theta}_{a1}^b = \frac{\cos \phi_{a1}^b + \cos \phi_{ab}^1 \cos \phi_{b1}^a}{\sin \phi_{ab}^1 \sin \phi_{b1}^a}$$

Range determined by the boundary data:

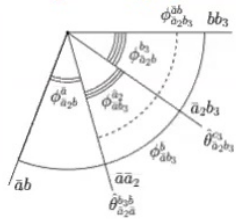
- >1 , Lorentzian, co-chronal (thick wedge)
- $[-1,1]$, Euclidean
- <-1 , Lorentzian, anti-chronal (thin wedge)

This definition depends on the edge chosen.

When the 2d angles match, the expression becomes independent of b , and defines a unique 4d angle

This is enough for simplices, whose edges are dual to 3-cycles.

But general graphs have edges dual to n -cycles, for which we cannot apply this formula



$$\cos \hat{\theta}_{a2a}^{b3b} := \frac{\cos \phi_{a2a}^{b3b} + \cos \phi_{a2a}^{\bar{a}} \cos \phi_{\bar{a}2a}^{b3b}}{\sin \phi_{a2a}^{\bar{a}} \sin \phi_{\bar{a}2a}^{b3b}}$$

Successive use of SCL shows that the 4d edge-dependent dihedral angles depends on all nodes entering the cycle

Again for angle-matching data, the definition is edge-independent and there is a unique 4d angle

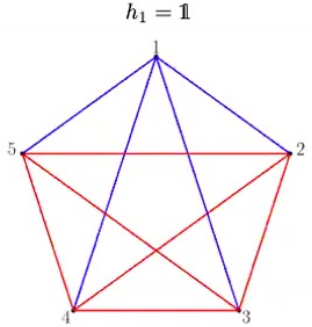
PI20.key

View Zoom Add Slide Play Keynote Live Table Chart Text Shape Media Comment Collaborate Format Animate Document

4-simplex asymptotics revisited

Eqs to solve: $H_a \vec{n}_{ab} = -H_b \vec{n}_{ba}$

$h_1 = 1$



Slide Layout

Blank

Change Master

Appearance

- ☐ Title
- ☐ Body
- ☐ Slide Number

Background

Edit Master Slide

PI20.key

View Zoom Add Slide Play Keynote Live Table Chart Text Shape Media Comment Collaborate Format Animate Document

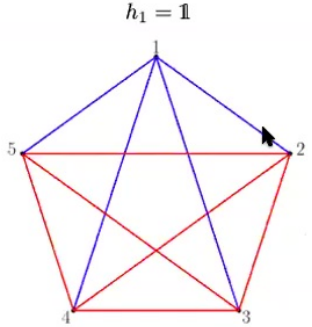
4-simplex asymptotics revisited

Eqs to solve: $H_a \vec{n}_{ab} = -H_b \vec{n}_{ba}$

- Look at eqs 1a:

$$\vec{n}_{1a} = -H_a \vec{n}_{a1}$$
- Use gauge freedom at node a to rotate normals antiparallel to 1:

$$\vec{n}_{1a} = -\vec{n}_{a1}$$



$h_1 = 1$

Slide Layout

Blank

Change Master

Appearance

☐ Title

☐ Body

☐ Slide Number

► Background

Edit Master Slide

PI20.key

View 96% Zoom Add Slide Play Keynote Live Table Chart Text Shape Media Comment Collaborate Format Animate Document

4-simplex asymptotics revisited

Eqs to solve: $H_a \vec{n}_{ab} = -H_b \vec{n}_{ba}$

- Look at eqs 1a:

$$\vec{n}_{1a} = -H_a \vec{n}_{a1} = H_a \vec{n}_{1a} \Leftrightarrow h_a = \pm \exp\left(\frac{i}{2} \omega_a \vec{n}_{a1} \cdot \vec{\sigma}\right)$$
 $\omega_a \in \mathbb{C}$
- Use gauge freedom at node a to rotate normals antiparallel to 1:

$$\vec{n}_{1a} = -\vec{n}_{a1}$$

All directions determined. Use remaining eqs ab to solve for ω_a

Slide Layout

Blank

Change Master

Appearance

☐ Title

☐ Body

☐ Slide Number

Background

Edit Master Slide

PI20.key

View 96% Zoom Add Slide Play Keynote Live Table Chart Text Shape Media Comment Collaborate Format Animate Document

4-simplex asymptotics revisited

Eqs to solve: $H_a \vec{n}_{ab} = -H_b \vec{n}_{ba}$

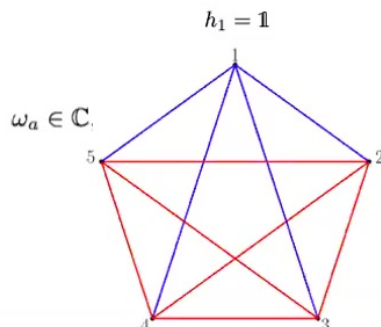
- Look at eqs 1a:

$$\vec{n}_{1a} = -H_a \vec{n}_{a1} = H_a \vec{n}_{1a} \Leftrightarrow h_a = \pm \exp\left(\frac{i}{2} \omega_a \vec{n}_{a1} \cdot \vec{\sigma}\right), \quad \omega_a \in \mathbb{C}$$
- Use gauge freedom at node a to rotate normals antiparallel to 1:

$$\vec{n}_{1a} = -\vec{n}_{a1}$$

All directions determined. Use remaining eqs ab to solve for ω_a

- Write $\vec{n}_{ab} = -H_a^{-1} H_b \vec{n}_{ba}$, compute explicit composition of 4-screws, take scalar projections:



Slide Layout

Blank

Change Master

Appearance

☐ Title

☐ Body

☐ Slide Number

Background

Edit Master Slide

PI20.key

View Zoom Add Slide Play Keynote Live Table Chart Text Shape Media Comment Collaborate Format Animate Document

Classifying the solutions

$$\cos(\omega_a + \bar{\xi}_{a1}^b) = \cos \hat{\theta}_{a1}^b, \quad \rightarrow \text{at most two solutions per each } \omega_a$$

$$\sin \phi_{b1}^a \sin(\omega_a + \bar{\xi}_{a1}^b) = \sin \phi_{a1}^b \sin(\omega_b + \bar{\xi}_{1b}^a) \quad \rightarrow \text{constrain the } \omega_a \text{ among themselves}$$

Write $\omega_a := \alpha_a + i\beta_a$

- Euclidean sector:** $\beta_a = 0 \quad \forall a \quad \Leftrightarrow H_a = R_a \in \text{SO}(3) \text{ for all nodes}$
 $\alpha_a = \pm \hat{\theta}_{a1}^b - \bar{\xi}_{a1}^b$

the + sign is always a solution for any vector geometry

the - sign is only a solution if angle-matching conditions hold

because all faces are triangles and areas match, this implies shape matching: Regge geometries
 finally, the second eqs imply that the signs must coincide for all a : **only two solutions in the end**

- Lorentzian sector:** $\alpha_a = -\bar{\xi}_{a1}^b + \Pi_{a1}$
 $\beta_a = \pm \hat{\theta}_{a1}^b \quad H_a \notin \text{SO}(3)$

solutions exist only if angle-matching conditions hold; no 'lorentzian vector geometries'

again, the second eqs imply that the signs must coincide for all a : **only two solutions in the end**

Slide Layout: Blank, Change Master

Appearance: ☐ Title, ☐ Body, ☐ Slide Number

Background:

Edit Master Slide

PI20.key

View Zoom Add Slide Play Keynote Live Table Chart Text Shape Media Comment Collaborate Format Animate Document

Holonomy-flux vs discrete geometries

Lee: we started with a nice and elegant representation of the gravitational field in terms of holonomies and fluxes; how did we end up in this intricate mess of discrete geometries with piles of dihedral angles?

It is actually a very relevant question, and I would like to offer my viewpoint here. There are two issues here that can be distinguished:

- first order vs second order formalism**
HF are variables for first-order formulation of gravity, with the connection as an independent variables when we do this, even in the continuum, we get a much simpler and elegant picture than EEs:

$$\star e \wedge F = 0, \quad d_\omega e = 0$$
polynomial equations. The intricacy of the Riemann tensor is not lost; it is hidden in the new dynamical equations. Solving them reintroduces the non-polynomiality
- truncations.** In the spin foam approach, but also in most canonical papers, we do calculations on a fixed graph. This introduces a truncation of the dofs of LQG, reducing them to a finite number. The dynamics of these dofs is under study; **one way to advance it is to interpret the dofs as discrete geometries, then use help from discrete models of GR to understand the quantum dynamics.** This leads to dihedral angles...

This is one approach to study the dynamics; it would be great if simpler descriptions were accessible

Slide Layout

Blank

Change Master

Appearance

☐ Title

☐ Body

☐ Slide Number

Background

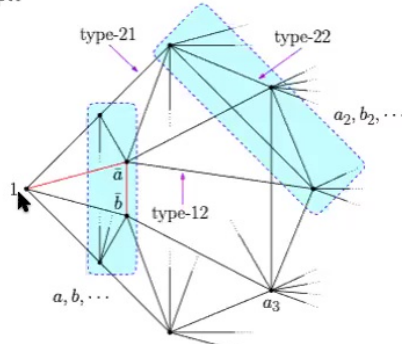
Edit Master Slide

PI20.key

View Zoom Add Slide Play Keynote Live Table Chart Text Shape Media Comment Collaborate Format Animate Document

The general algorithm

No need of invoking bivector reconstruction theorems, algebraic maps, commuting diagrams...
It all boils down to elementary trigonometry
the price to pay is that everything is gauge dependent. But interpreting the boundary data in terms of discrete geometries, there is an obvious gauge better than the others: the one where the edges are aligned
Benefit: can be applied to any graph



Proceed step by step:

- pick an initial node, determine all group elements at the nodes connected to it
- pick one of the first neighbours, and determine all unknown group elements connected to it
- continue until all group elements have been determined, and all link equations verified

the algorithm requires a choice of 'dominant node set' of the graph,
and uses a preferred gauge fixing at every node:
taking the normals antiparallel to those of the seed node of each step

Slide Layout

Blank

Change Master

Appearance

☐ Title

☐ Body

☐ Slide Number

► Background

Edit Master Slide

PI20.key

View Zoom Add Slide Play Keynote Live Table Chart Text Shape Media Comment Collaborate Format Animate Document

New features appearing beyond the 4-simplex

- As anticipated by revisiting the 4-simplex analysis, the true conditions for the existence of distinct critical points are angle-matching; the fact that for the 4-simplex they imply Regge data is a consequence of the fact that all faces are triangular
- For more general graphs, boundary data with distinct critical points are conformal twisted geometries (first pointed out by Bahr-Steinhaus from examples in the Euclidean EPRL-KKL model)
- 3d Regge geometries, and flat-embeddable 3d Regge geometries that define 4d Regge geometries, are subsets with the same number of critical points
- More than two critical points are possible for modular graphs (first pointed out by Bahr)
- Beautiful interplay between spherical cosine laws and critical point equations, for any n -cycle
In fact, one can *learn* about generalised SCL, or Lorentzian trigonometry, studying these eqs

0 Generic data (twisted geometries)	1 Vector geometries
≥ 2 Lor. angle-matched	≥ 2 Eucl. angle-matched
≥ 2 Lor. 3d Regge	≥ 2 Eucl. 3d Regge
≥ 2 Lor. flat polytopes	≥ 2 Eucl. flat polytopes

View 96 % + +

Play Keynote Live

Table Chart Text Shape Media Comment

Collaborate

Format Animate Document

General asymptotic formulas

- For vector data, 1 critical point:
$$A_\Gamma = \frac{(2\pi)^{3(N-1)} 2^{2L+N-1} J}{\lambda^{3(N-1)}} e^{i\Psi} \frac{\Omega^{(+)} }{\sqrt{\det -H^{(+)}}} + O(\lambda^{-3N+2})$$

For angle-matched data, we can define an edge-independent 4d dihedral angle from spherical cosine laws, and a action

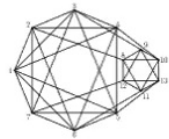
$$S_\Gamma(j_{ab}, \phi_{ab}^c) := \sum_{(ab)} j_{ab} \theta_{ab}(\phi)$$

- For angle-matched twisted geometries, on non-modular graphs, 2 critical points:

Euclidean
$$A_\Gamma = \frac{(2\pi)^{3(N-1)} 2^{2L+N-1} J}{\lambda^{3(N-1)}} e^{i\Psi} \left(\frac{\Omega^{(+)} e^{i\lambda S_\Gamma}}{\sqrt{\det -H^{(+)}}} + \frac{\Omega^{(-)} e^{-i\lambda S_\Gamma}}{\sqrt{\det -H^{(-)}}} \right) + O(\lambda^{-3N+2})$$

Lorentzian
$$A_\Gamma = \frac{(2\pi)^{3(N-1)} 2^{2L+N-1} J}{\lambda^{3(N-1)}} (-1)^\chi e^{i\Psi} \left(\frac{\Omega^{(+)} e^{i\lambda \gamma S_\Gamma}}{\sqrt{\det -H^{(+)}}} + \frac{\Omega^{(-)} e^{-i\lambda \gamma S_\Gamma}}{\sqrt{\det -H^{(-)}}} \right) + O(\lambda^{-3N+2})$$

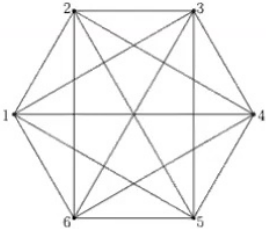
- On n-modular graphs, up to 2^n critical points. E.g. Euclidean:

$$A_\Gamma = \frac{(2\pi)^{3(N-1)} 2^{2L+N-1} J}{\lambda^{3(N-1)}} e^{i\Psi} \sum_{\epsilon_i = \pm} \frac{\Omega^{(\epsilon_i)}}{\sqrt{\det -H^{(\epsilon_i)}}} e^{i\lambda S_\Gamma^{(\epsilon_i)}[i]}$$


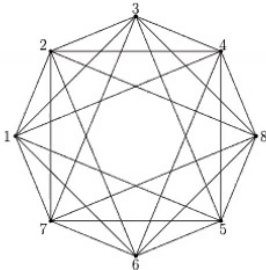
PI20.key

View Zoom Add Slide Play Keynote Live Table Chart Text Shape Media Comment Collaborate Format Animate Document

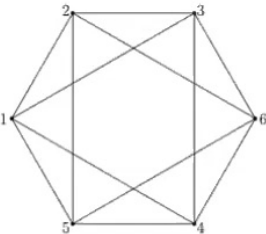
Graphs explicitly solved, and new features they exemplify



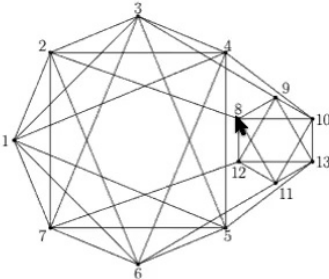
appearance of conformal twisted geometries



second neighbours



no polytope boundary data



non-minimal cycles
modular graph

Slide Layout

Blank

Change Master

Appearance

☐ Title

☐ Body

☐ Slide Number

► Background

Edit Master Slide

PI20.key

View Zoom Add Slide Play Keynote Live Table Chart Text Shape Media Comment Collaborate Format Animate Document

Summary of results

- **Asymptotics analysis of the EPRL model on any vertex graph possible**
- Among the graphs and data with 4d interpretation, 4-simplex is the dominant one (slowest power law decay)
- There are more general geometries than Regge's with distinct critical points

$$S_{\Gamma}(j_{ab}, \phi_{ab}^c) := \sum_{(ab)} j_{ab} \theta_{ab}(\phi)$$

- Apart from the mathematical results, what physical implications?
- The fact that the EPRL model has more general geometries on a general vertex is not a surprise after all the simplicity constraints it implements are a complete discretization of the continuum ones only for a 4-simplex
- Bahr and Belov for instance are exploring a modification of the model that could implement additional constraints
- The question of removing some critical boundary data resonates with other ideas to restrict also the 4-simplex amplitude (Engle, Zipfel, Han...)
- Asante-Dittrich-Haggard are exploring the dependence of the dynamics on the strength with which the shape matching conditions are imposed
- Of course, the validity of the semiclassical limit requires more stringent questions (dynamics on internal faces, cosine contributions, vector geometries, etc...)
- **All these are interesting open questions for future work**

When I first asked myself this question, shortly after the KKL extension, the answer appeared immediately not easy. Clearly, new techniques were needed.

These techniques now exist, and hopefully they can be useful to the study of the EPRL model and of LQG more in general

Slide Layout

Blank

Change Master

Appearance

☐ Title

☐ Body

☐ Slide Number

► Background

Edit Master Slide